

***Electronic Supplementary Information***

**Synthesis and Evaluation of Porous Azo-Linked Polymers for  
Carbon Dioxide Capture and Separation**

Pezhman Arab, Emily Parrish, Timur Islamoglu, and Hani M. El-Kaderi\*

Department of Chemistry, Virginia Commonwealth University, Richmond, Virginia 23284-  
2006, United States

\*To whom correspondence should be addressed. Email: helkaderi@vcu.edu

## Contents

	<i>Page</i>
<i>Table S1 (optimization of catalyst amount for ALP-7)</i>	<b>S3</b>
<i>FT-IR spectroscopy analysis</i>	<b>S4-S7</b>
<i>Solid state <math>^{13}\text{C}</math> CP-MAS NMR analysis</i>	<b>S8-S11</b>
<i>Scanning electron microscopy (SEM) imaging</i>	<b>S12-S13</b>
<i>Powder X-ray diffraction (XRD) analysis</i>	<b>S14</b>
<i>Thermogravimetric analysis (TGA)</i>	<b>S15</b>
<i>BET plots</i>	<b>S16</b>
<i>Langmuir plots</i>	<b>S17</b>
<i>Pore size distribution of ALPs</i>	<b>S18</b>
<i>Low pressure (0 – 1.0 bar) gas uptake isotherms of ALPs at 298 K</i>	<b>S19</b>
<i>Table S2 (comparison of porosity parameters of ALPs)</i>	<b>S20</b>
<i>Table S3 (gas uptakes and <math>Q_{st}</math> of ALPs)</i>	<b>S21</b>
<i>Table S4 (comparison of porous azo-linked polymers for <math>\text{CO}_2</math> capture)</i>	<b>S22</b>
<i>Virial fittings</i>	<b>S23-S24</b>
<i>Langmuir-Freundlich fittings for gas isotherms</i>	<b>S25-S28</b>
<i>High-pressure (1-10 bar) gas uptake of ALPs at 298 K</i>	<b>S29-S30</b>
<i>Table S5 (IAST selectivity of different classes of azo-linked porous polymers)</i>	<b>S31</b>
<i>Initial slope selectivity studies of ALPs</i>	<b>S32-S36</b>

**Table S1.** The effect of amount of catalyst on surface area of ALP-7.<sup>a</sup>

Entry	CuBr (mg)	Pyridine (mg)	Surface area (m <sup>2</sup> g <sup>-1</sup> ) <sup>b</sup>
1	20	80	60
2	40	160	400
3	80	320	100
4	80	160	390
5	60	160	380
6	60	120	240
7	40	120	370
8	30	80	230

<sup>a</sup>Reaction conditions: monomer (100 mg), THF (11 ml), toluene (11 ml), stirred at 25 °C for 24 h, at 60 °C for 12 h, and at 80 °C for 12 h. <sup>b</sup>BET surface areas were calculated from N<sub>2</sub> adsorption isotherms collected by NOVA (*Quantachrome*).

**Fig. S1** FT-IR spectra of ALP-5 and its corresponding monomer (TASBF).

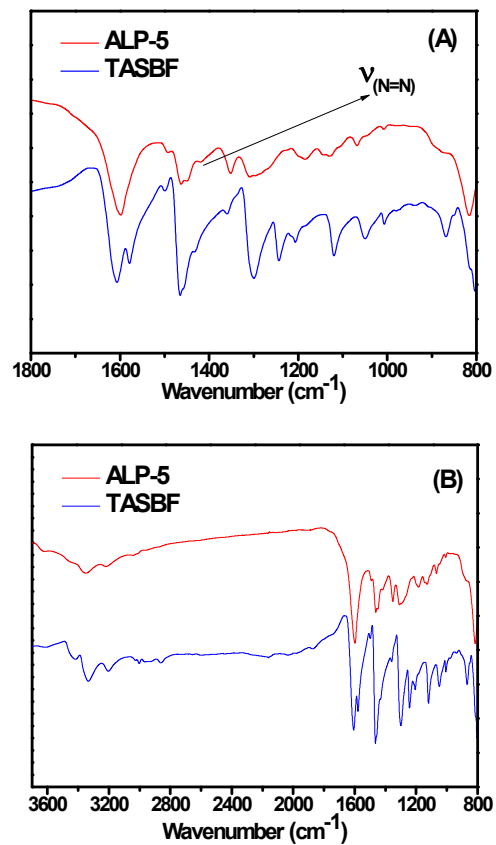


**Fig. S2** FT-IR spectra of ALP-6 and its corresponding monomer (TAPPA).

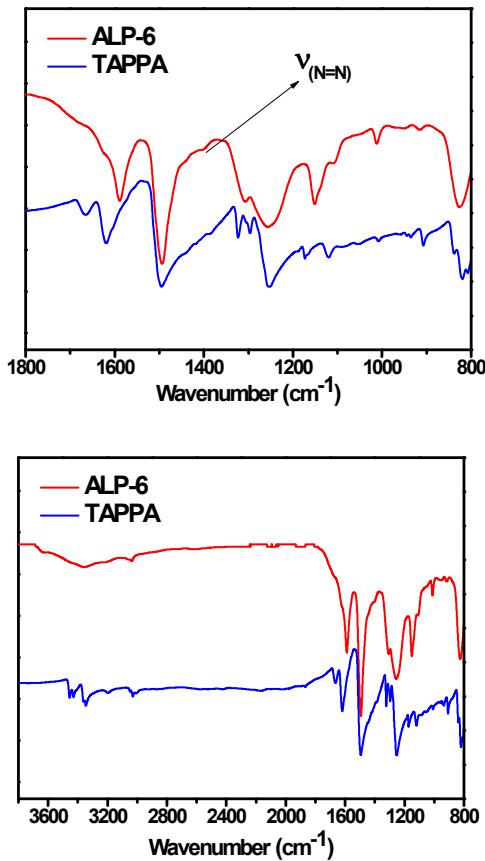


**Fig. S3** FT-IR spectra of ALP-7 and its corresponding monomer (TAPA).

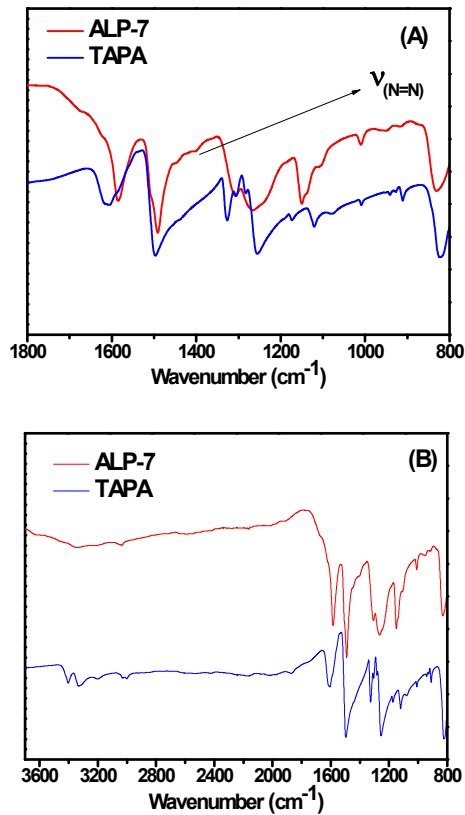


**Fig. S4** FT-IR spectra of ALP-8 and its corresponding monomer (TAPE).

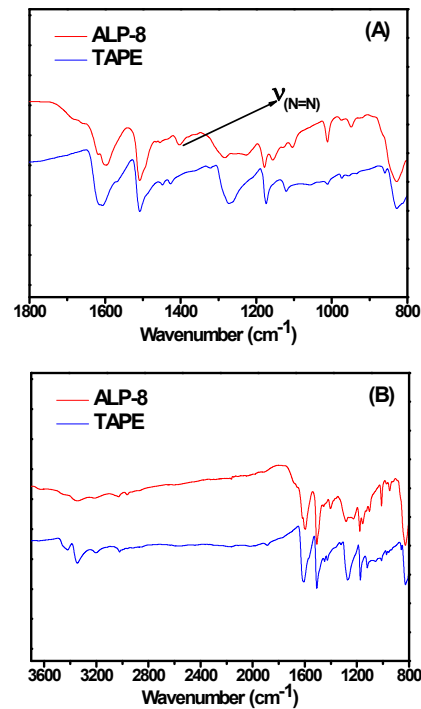


**Fig. S5** Solid state  $^{13}\text{C}$  CP-MAS NMR spectrum of ALP-5. Asterisks denote spinning side-bands.

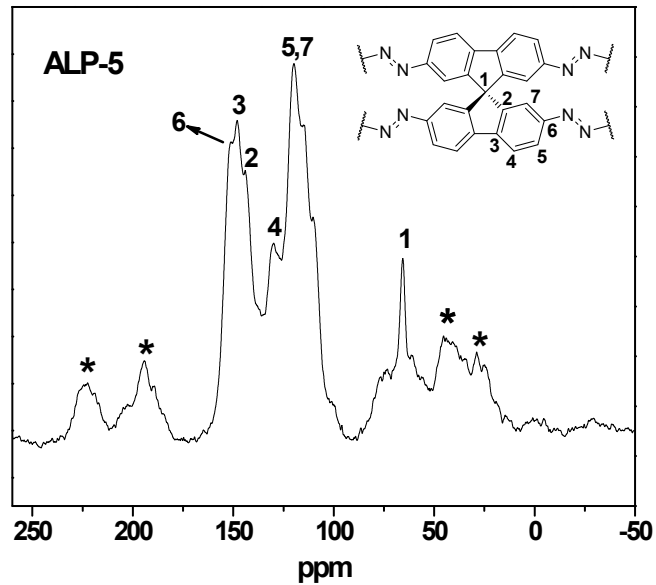


**Fig. S6** Solid state  $^{13}\text{C}$  CP-MAS NMR spectrum of ALP-6. Asterisks denote spinning side-bands.

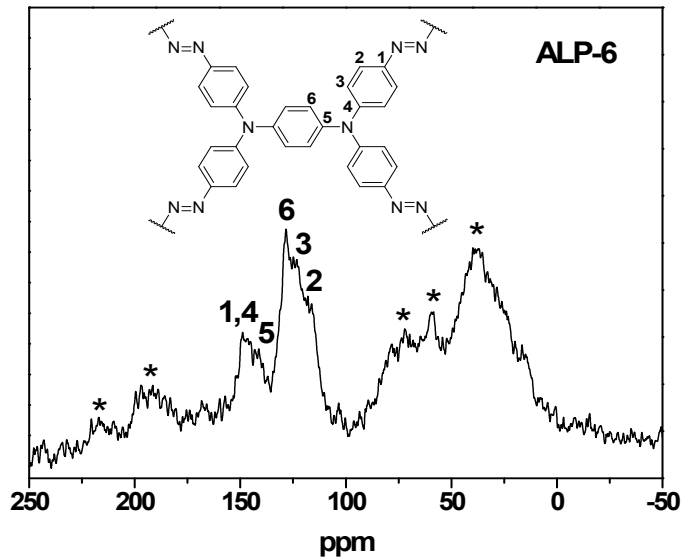


**Fig. S7** Solid state  $^{13}\text{C}$  CP-MAS NMR spectrum of ALP-7. Asterisks denote spinning side-bands.

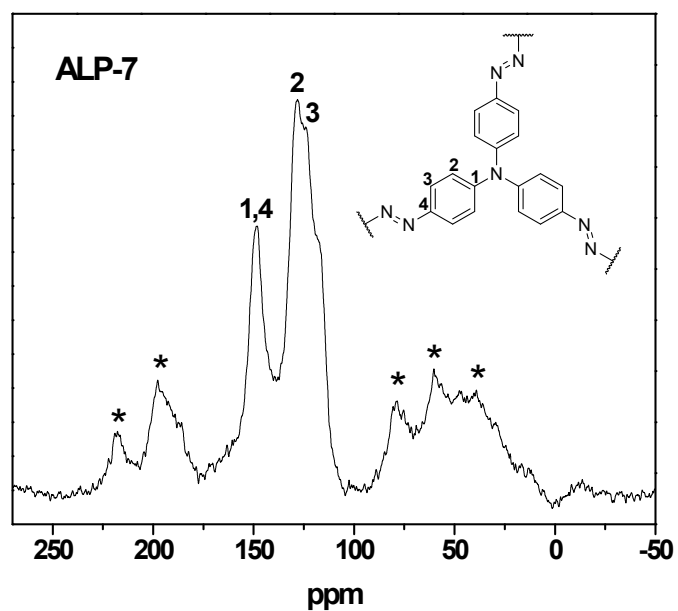


**Fig. S8** Solid state  $^{13}\text{C}$  CP-MAS NMR spectrum of ALP-8. Asterisks denote spinning side-bands.

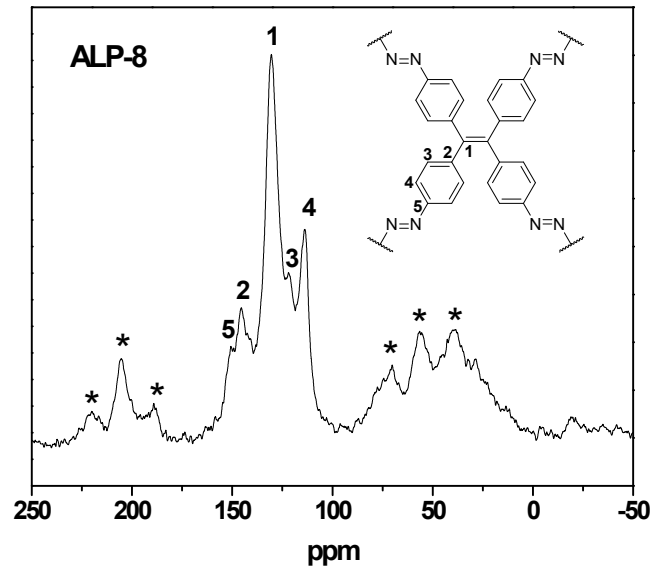


**Fig. S9** SEM image of ALP-5.

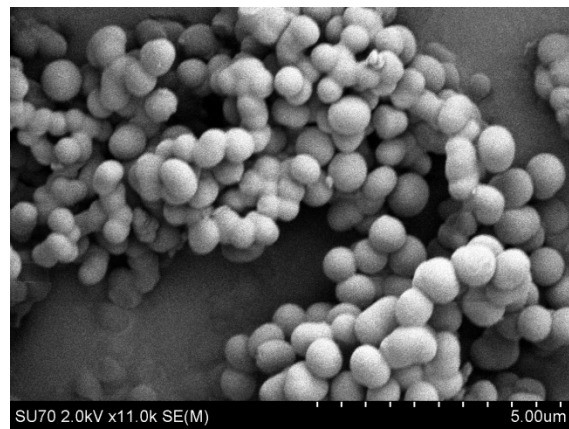


**Fig. S10** SEM image of ALP-6.

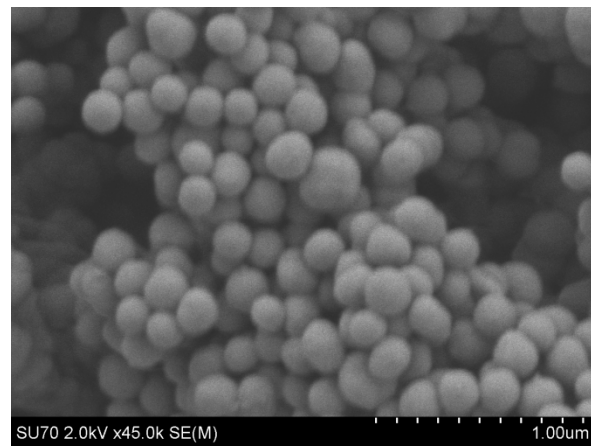


**Fig. S11** SEM image of ALP-7.

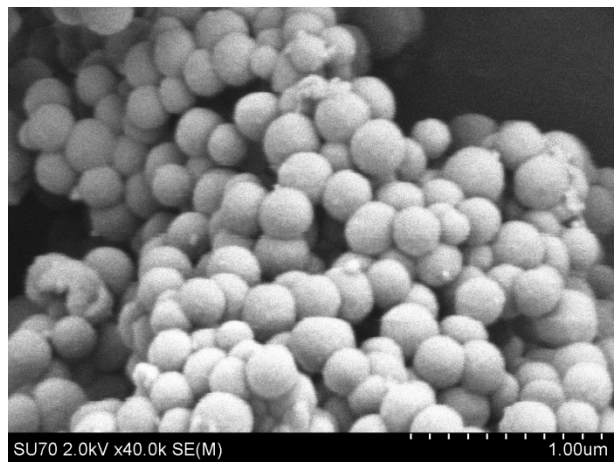


**Fig. S12** SEM image of ALP-8.

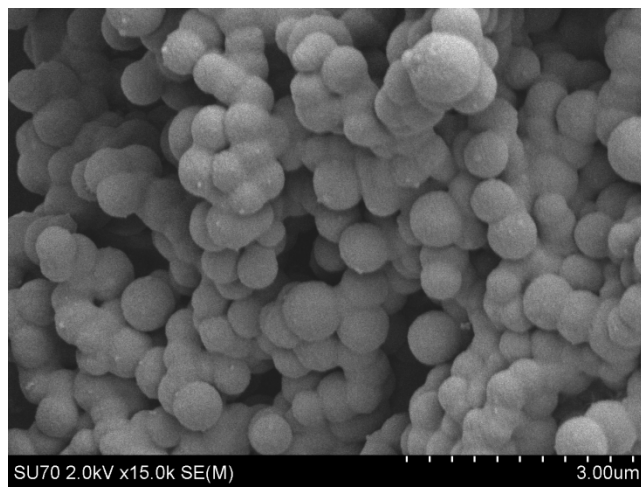


**Fig. S13** PXRD pattern of ALPs.

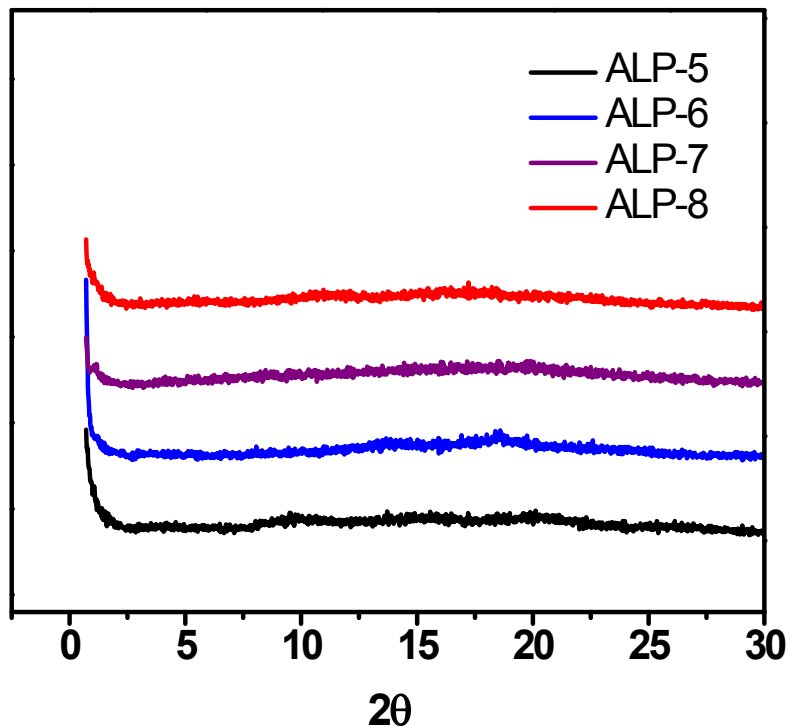


**Fig. S14** TGA traces of ALPs.

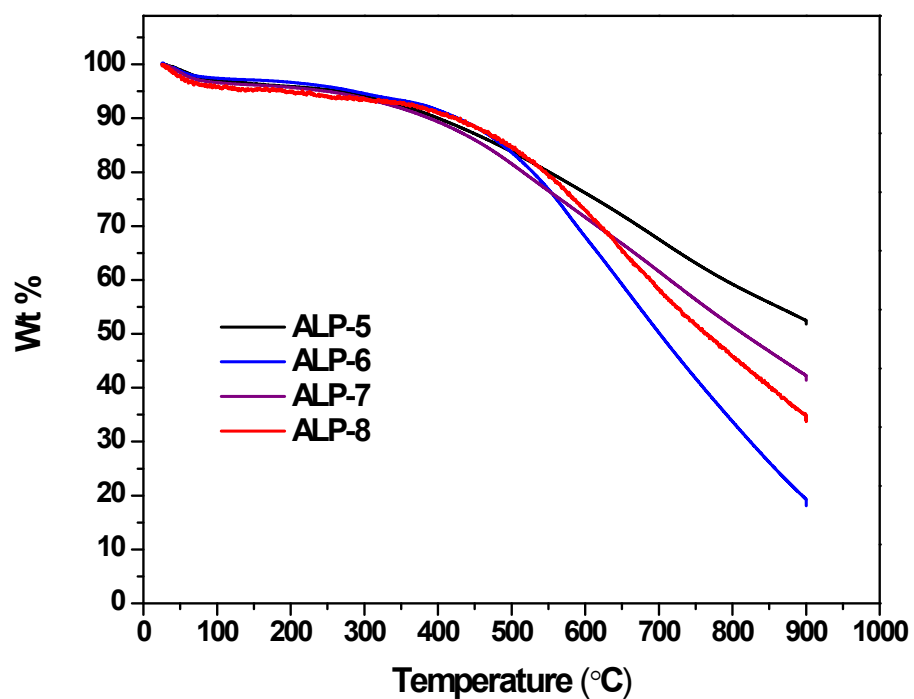


**Fig. S15** BET plots for ALPs.

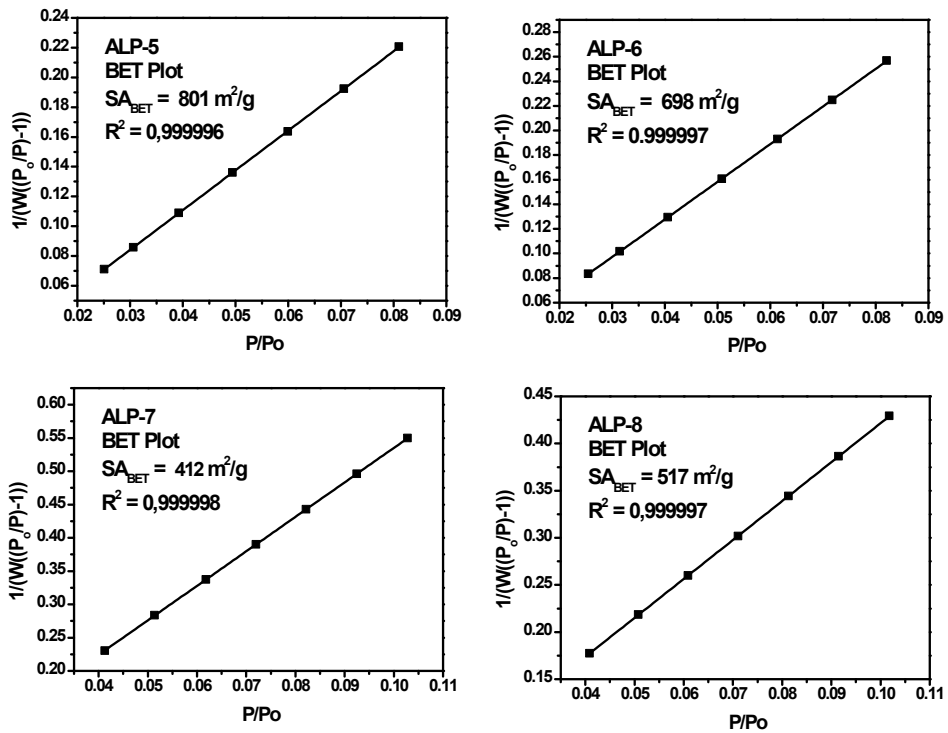


**Fig. S16** Langmuir plots for ALPs.

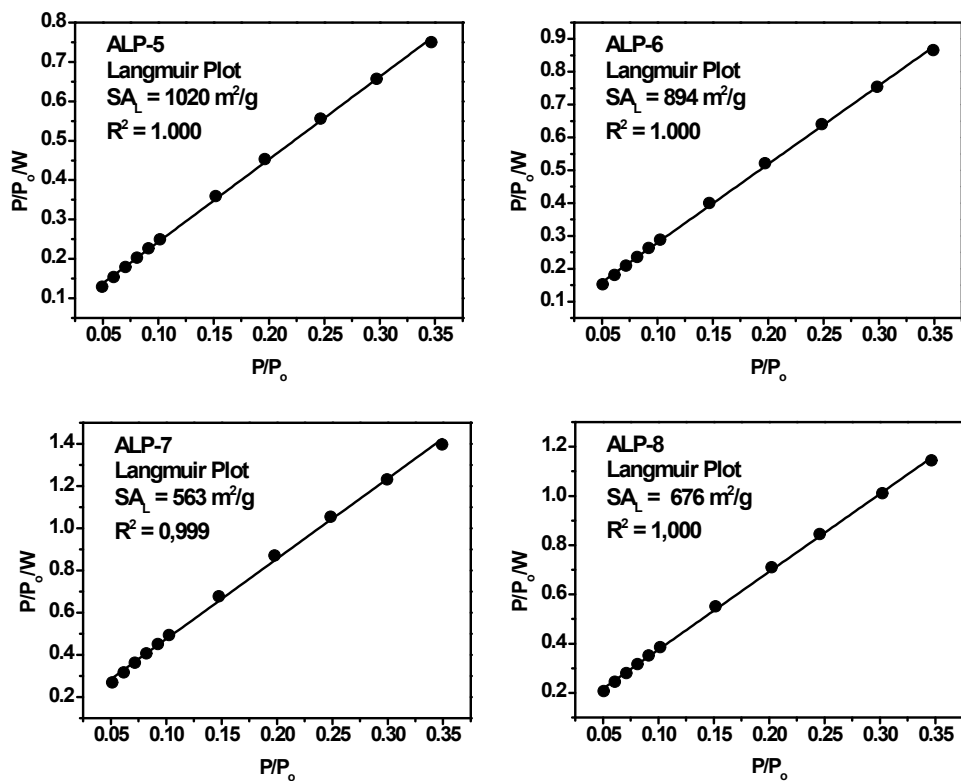


**Fig. S17** Pore size distribution of ALPs calculated from Ar adsorption branch using NLDFT (spherical/cylindrical model).

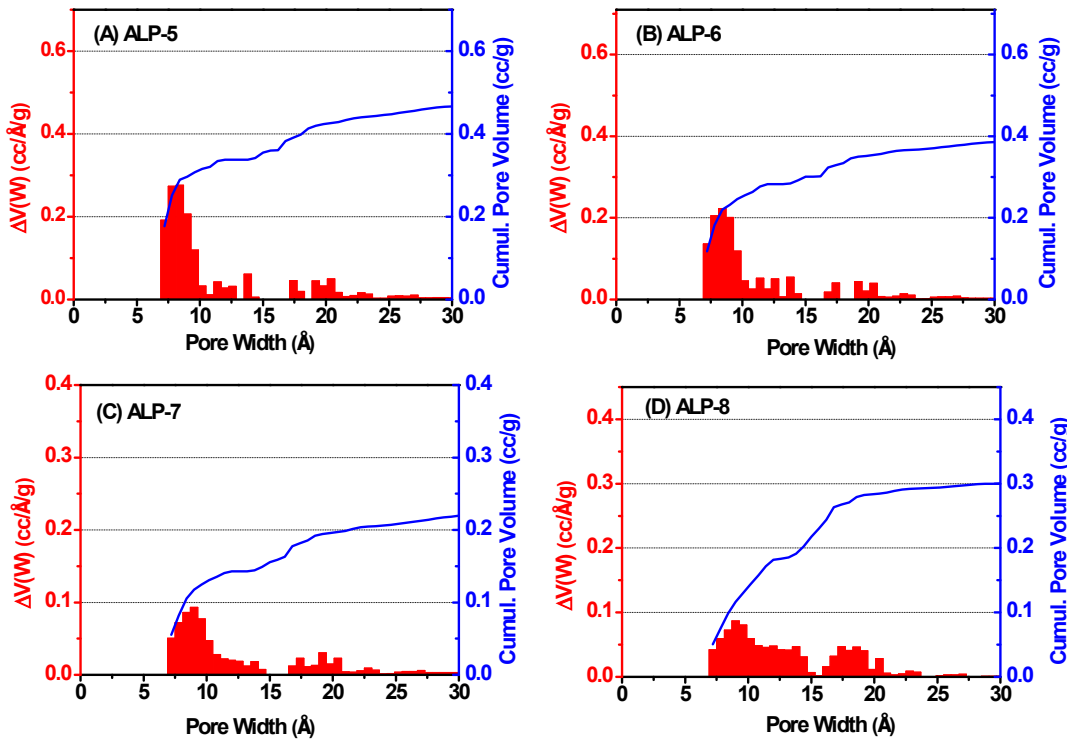


**Fig. S18** CO<sub>2</sub>, CH<sub>4</sub>, and N<sub>2</sub> adsorption isotherms of ALPs at 298 K.

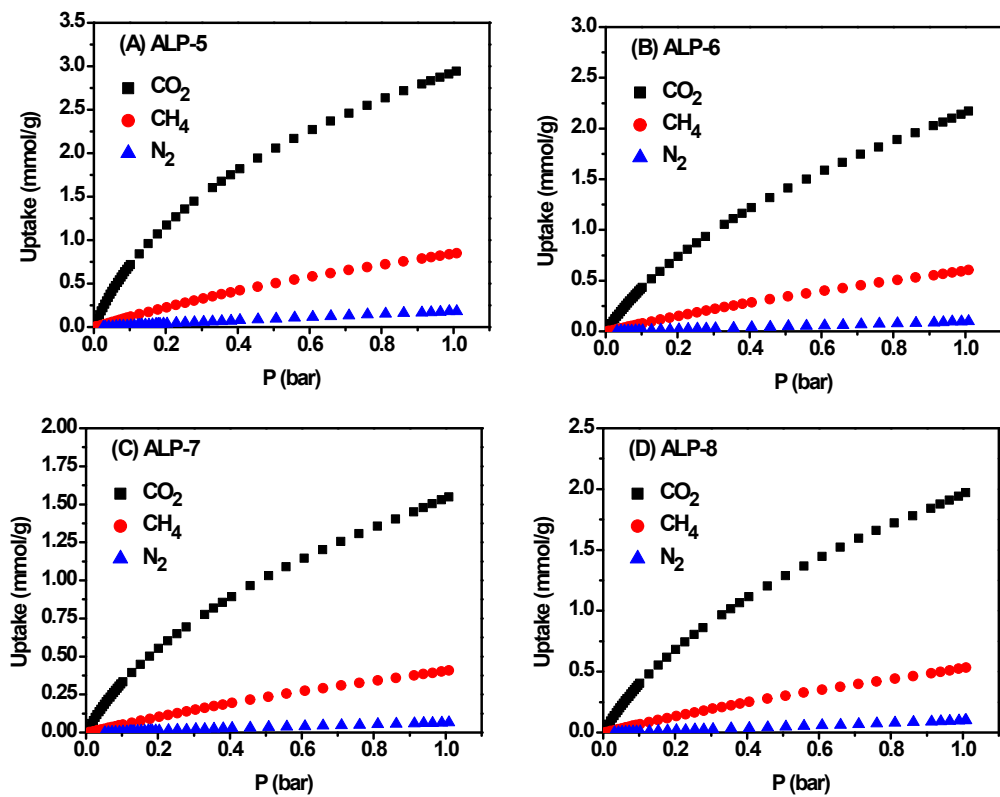


**Table S2.** Porosity parameters for ALPs.

Polymer	SA <sub>BET</sub> <sup>a</sup>	Dominant pore size (nm) <sup>b</sup>	Total Pore Volume <sup>c</sup>	Ref.
ALP-1	1235	1.0	0.66	<sup>1</sup>
ALP-2	1065	1.1	0.57	<sup>1</sup>
ALP-3	975	1.3	0.63	<sup>1</sup>
ALP-4	862	1.1	0.50	<sup>1</sup>
ALP-5	801	0.80	0.39	This Work
ALP-6	698	0.85	0.36	This Work
ALP-7	412	0.90	0.27	This Work
ALP-8	517	0.92	0.25	This Work

<sup>a</sup>Surface area ( $\text{m}^2 \text{ g}^{-1}$ ) calculated from the Ar adsorption branch according to the BET model. <sup>b</sup>Pore size distributions (PSDs) were estimated from the adsorption branch of the Ar isotherms by NLDFT. <sup>c</sup>The total pore volume ( $\text{cm}^3 \text{ g}^{-1}$ ) calculated from single point Ar uptake at  $P/P_0 = 0.90$ .

**Table S3.** CO<sub>2</sub>, CH<sub>4</sub>, and N<sub>2</sub> uptakes, and isosteric heats of adsorption ( $Q_{st}$ ) for ALPs.

Polymer	CO <sub>2</sub> Uptake at 1 bar <sup>a</sup>			CH <sub>4</sub> Uptake at 1 bar <sup>a</sup>			N <sub>2</sub> Uptake at 1 bar <sup>a</sup>		Ref.
	273 K	298 K	$Q_{st}$ <sup>b</sup>	273 K	298 K	$Q_{st}$ <sup>b</sup>	273 K	298 K	
ALP-1	5.4	3.3	29.2	1.6	0.94	20.8	0.41	0.21	1
ALP-2	4.8	2.4	27.9	1.1	0.67	18.5	0.31	0.14	1
ALP-3	3.8	2.3	29.6	1.1	0.60	21.0	0.25	0.12	1
ALP-4	3.5	1.8	28.2	0.89	0.52	21.2	0.24	0.12	1
ALP-5	4.5	2.9	32.5	1.4	0.85	22.4	0.40	0.18	This Work
ALP-6	3.4	2.2	28.6	1.0	0.60	19.0	0.25	0.10	This Work
ALP-7	2.5	1.5	30.7	0.73	0.40	22.2	0.19	0.06	This Work
ALP-8	3.0	2.0	29.4	0.90	0.53	20.0	0.21	0.10	This Work

<sup>a</sup>Uptake in mmol g<sup>-1</sup>. <sup>b</sup>Isosteric enthalpies of adsorption ( $Q_{st}$ ) in kJ mol<sup>-1</sup>at zero coverage.

**Table S4.** Surface area, CO<sub>2</sub> uptake, and isosteric heat of adsorption of porous azo-linked polymers.

Polymer	Surface area <sup>a</sup>	CO <sub>2</sub> uptake at 1 bar <sup>b</sup>		$Q_{st}$ for CO <sub>2</sub> <sup>c</sup>	Reference
		273 K	298 K		
ALP-1	1235	5.4	3.3	29.2	1
ALP-2	1065	4.8	2.4	27.9	1
ALP-3	975	3.8	2.3	29.6	1
ALP-4	862	3.5	1.8	28.2	1
ALP-5	801	4.5	2.9	32.5	This Work
ALP-6	698	3.4	2.2	28.6	This Work
ALP-7	412	2.5	1.5	30.7	This Work
ALP-8	517	3.0	2.0	29.4	This Work
azo-COP-1	635	2.4	1.5	29.3	2
azo-COP-2	729	2.6	1.5	24.8	2
azo-COP-3	493	1.9	1.2	32.1	2
azo-POF-1	712	3.0	1.9	27.5	3
azo-POF-2	439	1.9	1.3	26.6	3

<sup>a</sup>Surface area (m<sup>2</sup> g<sup>-1</sup>) calculated based on the BET model. <sup>b</sup>CO<sub>2</sub> uptake in mmol g<sup>-1</sup>. <sup>c</sup>Isosteric heat of adsorption ( $Q_{st}$ ) at zero coverage in kJ mol<sup>-1</sup>.

**Fig. S19** Virial fitting for CO<sub>2</sub> isotherms of ALPs.

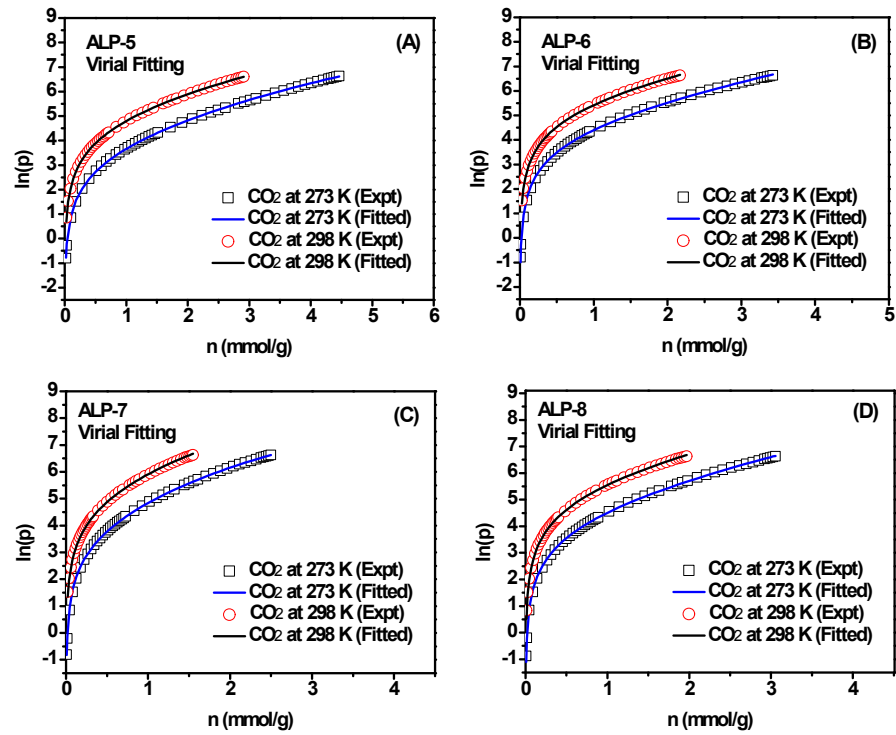


**Fig. S20** Virial fitting for  $\text{CH}_4$  isotherms of ALPs.

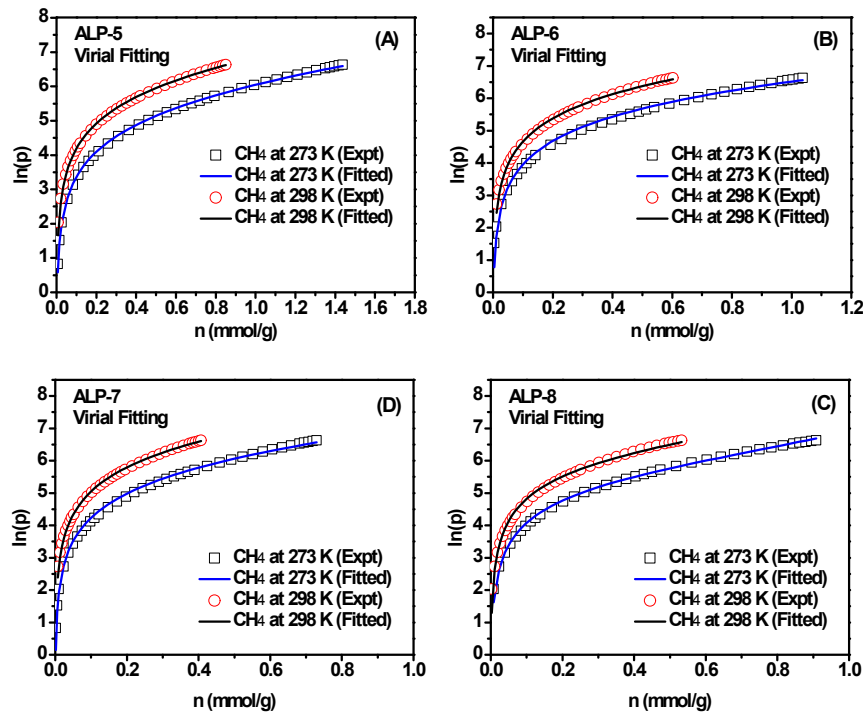


**Fig. S21** Experimental data and corresponding fittings of gas isotherms for ALP-5. (Dual site Langmuir-Freundlich for CO<sub>2</sub>, and single site Langmuir-Freundlich for CH<sub>4</sub> and N<sub>2</sub> with temperature dependent parameter at 273 and 298 K).

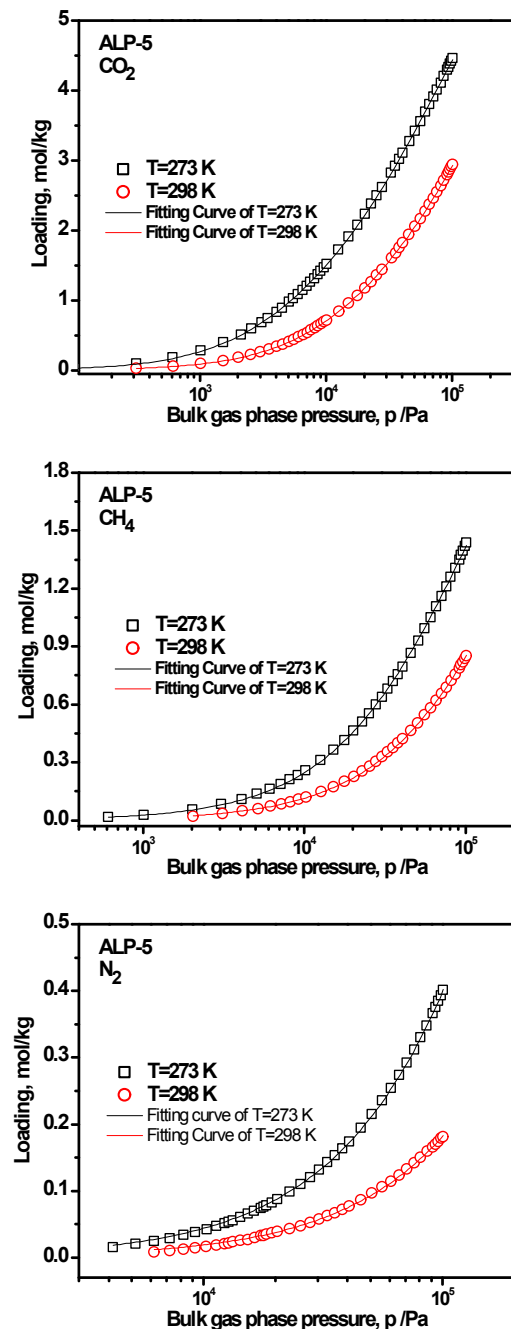




**Fig. S22** Experimental data and corresponding fittings of gas isotherms for ALP-6. (Dual site Langmuir-Freundlich for CO<sub>2</sub>, and single site Langmuir-Freundlich for CH<sub>4</sub> and N<sub>2</sub> with temperature dependent parameter at 273 and 298 K).

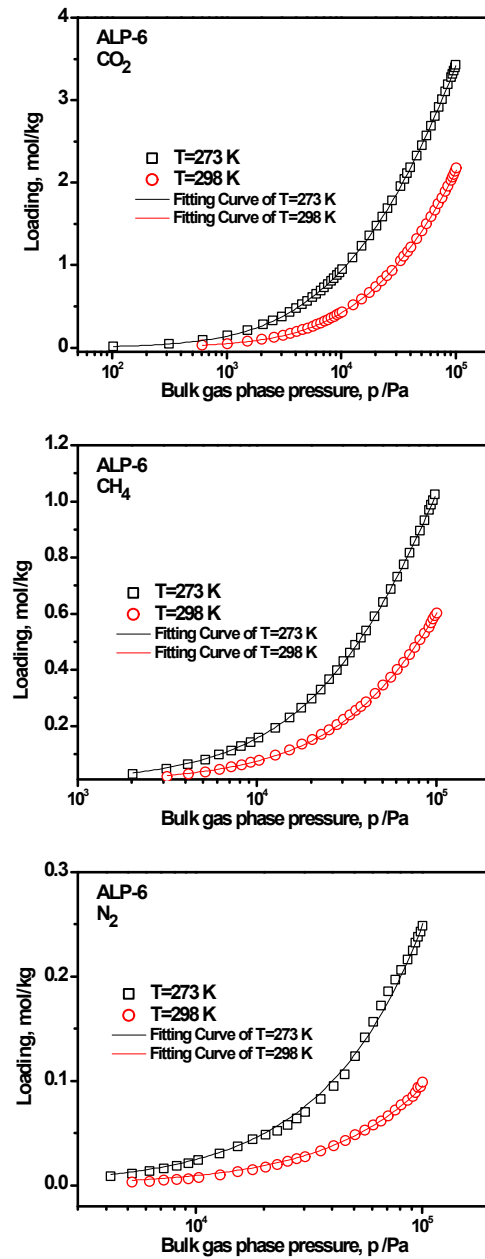


**Fig. S23** Experimental data and corresponding fittings of gas isotherms for ALP-7. (Dual site Langmuir-Freundlich for CO<sub>2</sub>, and single site Langmuir-Freundlich for CH<sub>4</sub> and N<sub>2</sub> with temperature dependent parameter at 273 and 298 K).

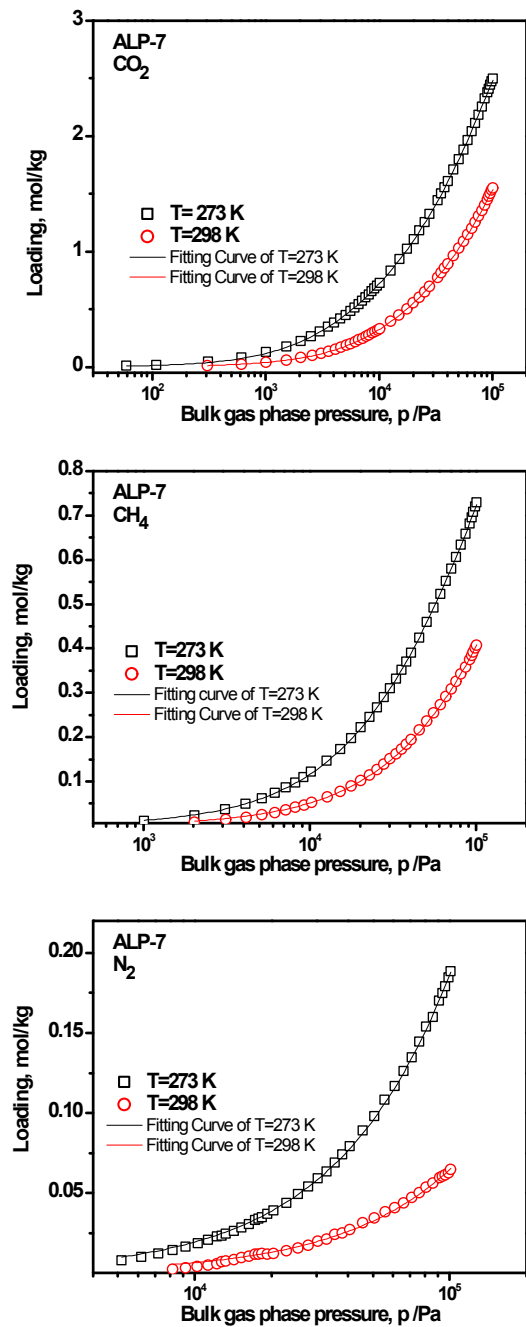


**Fig. S24** Experimental data and corresponding fittings of gas isotherms for ALP-8. (Dual site Langmuir-Freundlich for CO<sub>2</sub>, and single site Langmuir-Freundlich for CH<sub>4</sub> and N<sub>2</sub> with temperature dependent parameter at 273 and 298 K).

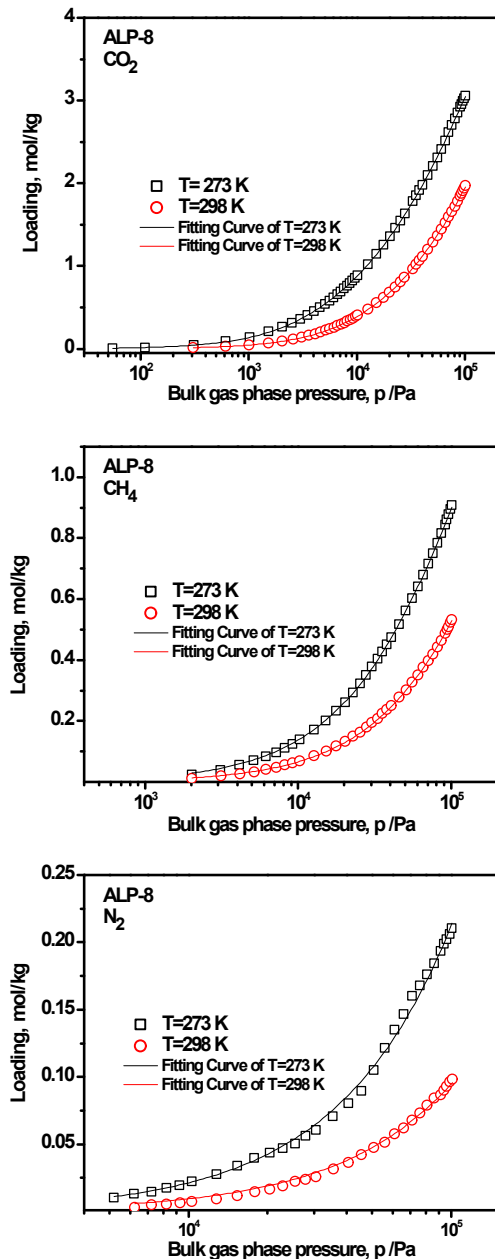


**Fig. S25** High-pressure total (absolute) CO<sub>2</sub> uptake of ALP-1 and ALP-5 at 298 K.

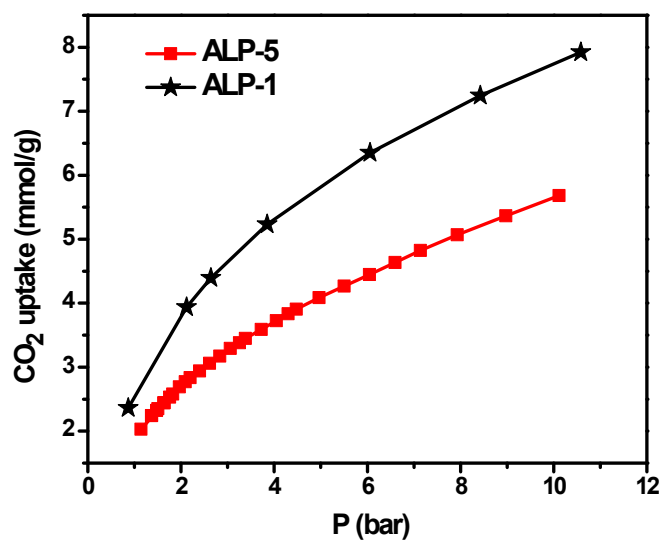


**Fig. S26** High pressure total (absolute)  $\text{CH}_4$  uptake of ALP-1 and ALP-5 at 298 K.

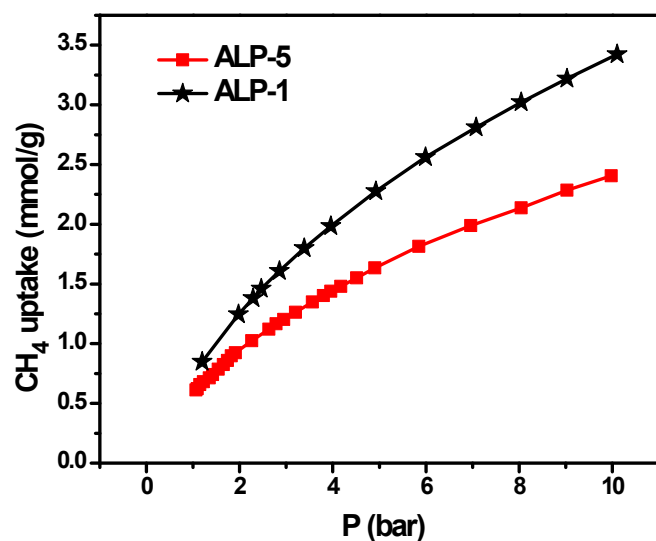


**Table S5.** IAST selectivity of different classes of azo-linked porous polymers.

Polymer	CO <sub>2</sub> /N <sub>2</sub> selectivity at 1 bar		Reference
	273 K	298 K	
ALP-1 <sup>a</sup>	40	28	<sup>1</sup>
ALP-2 <sup>a</sup>	34	26	<sup>1</sup>
ALP-3 <sup>a</sup>	44	35	<sup>1</sup>
ALP-4 <sup>a</sup>	35	26	<sup>1</sup>
ALP-5 <sup>b</sup>	60	47	This Work
ALP-6 <sup>b</sup>	45	48	This Work
ALP-7 <sup>b</sup>	52	56	This Work
ALP-8 <sup>b</sup>	51	44	This Work
azo-COP-1 <sup>a</sup>	64	97	<sup>2</sup>
azo-COP-2 <sup>a</sup>	110	131	<sup>2</sup>
azo-COP-3 <sup>a</sup>	79	96	<sup>2</sup>
azo-POF-1 <sup>a</sup>	52	37	<sup>3</sup>
azo-POF-2 <sup>a</sup>	55	42	<sup>3</sup>

<sup>a</sup>For CO<sub>2</sub>:N<sub>2</sub> mole ratio of 15:85. <sup>b</sup>For CO<sub>2</sub>:N<sub>2</sub> mole ratio of 10:90.

**Fig. S27** Gas uptakes and initial slope selectivity studies of ALP-5.

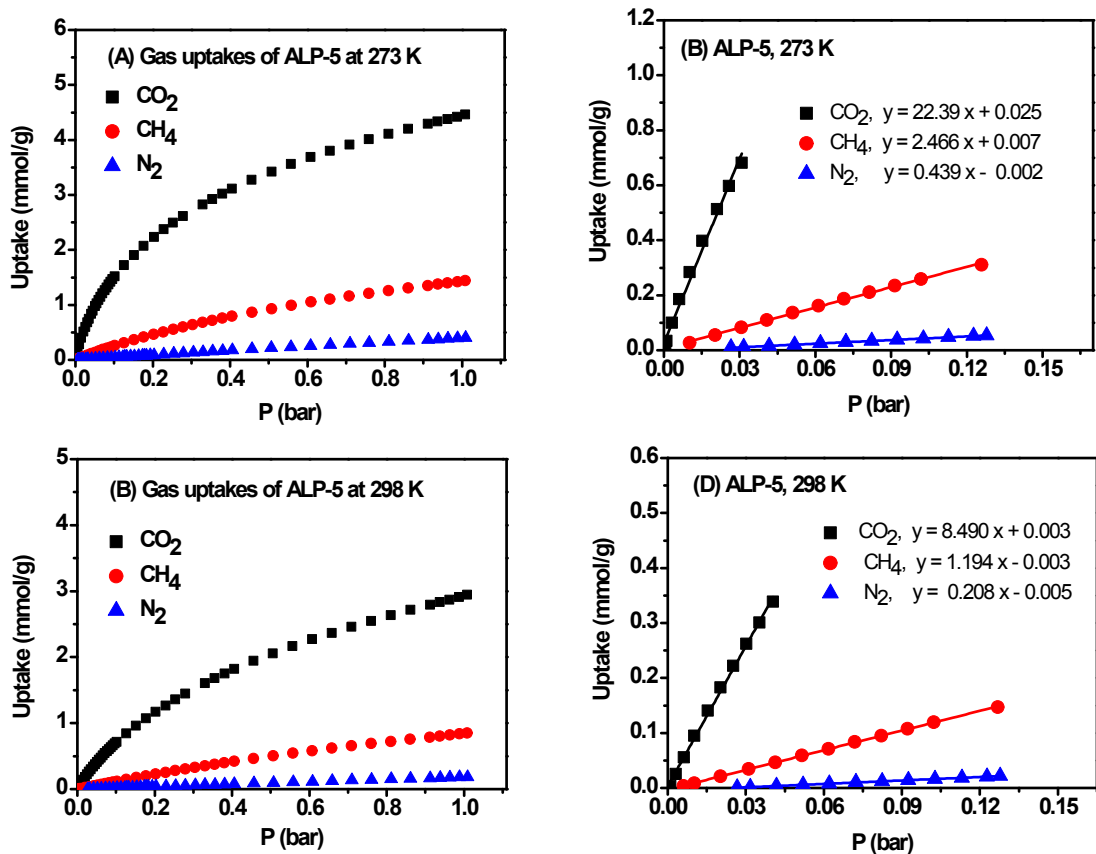


**Fig. S28** Gas uptakes and initial slope selectivity studies of ALP-6.

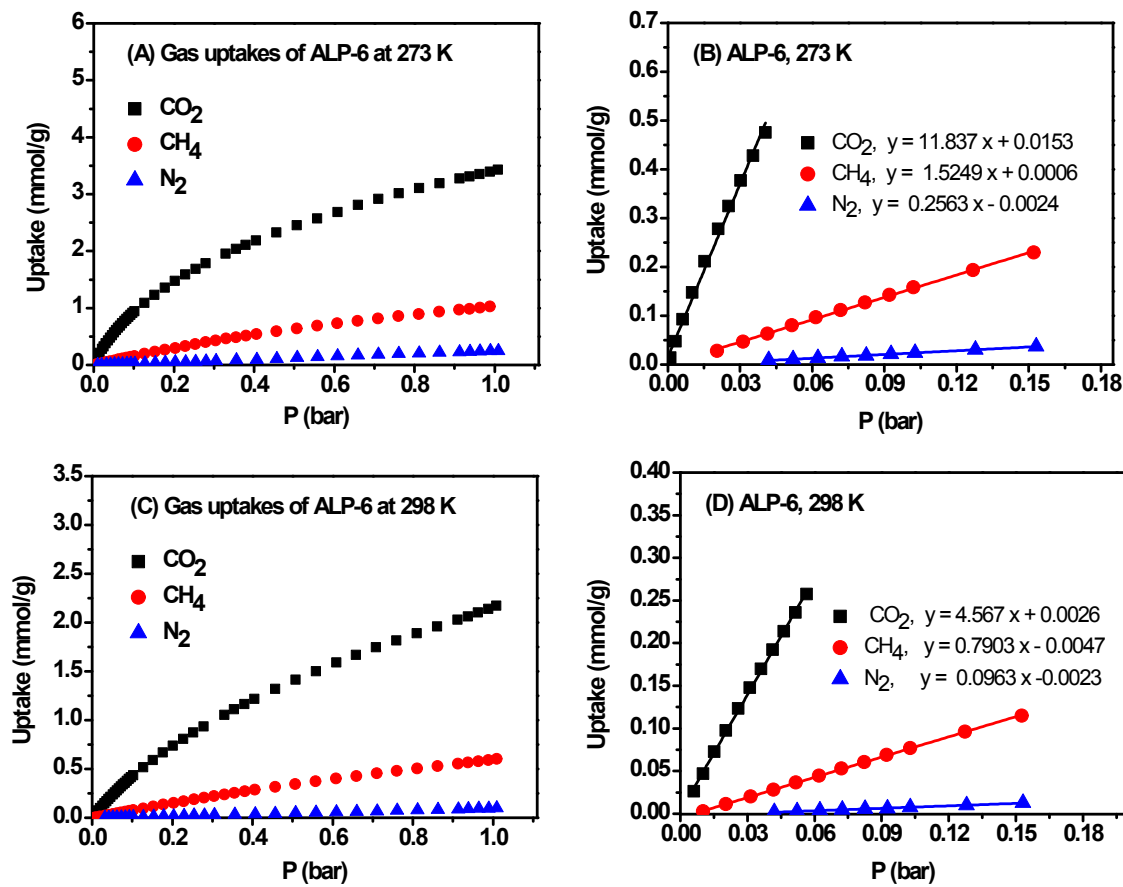


**Fig. S29** Gas uptakes and initial slope selectivity studies of ALP-7.

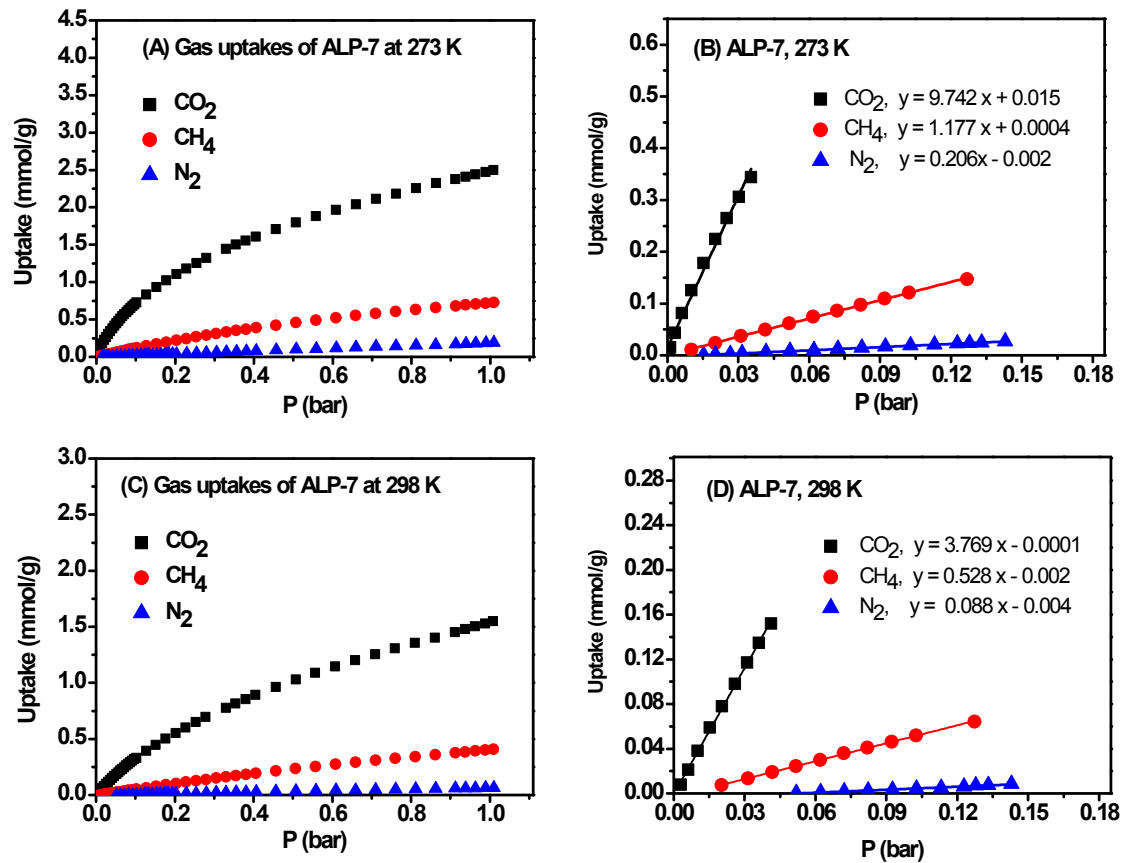


**Fig. S30** Gas uptakes and initial slope selectivity studies of ALP-8.

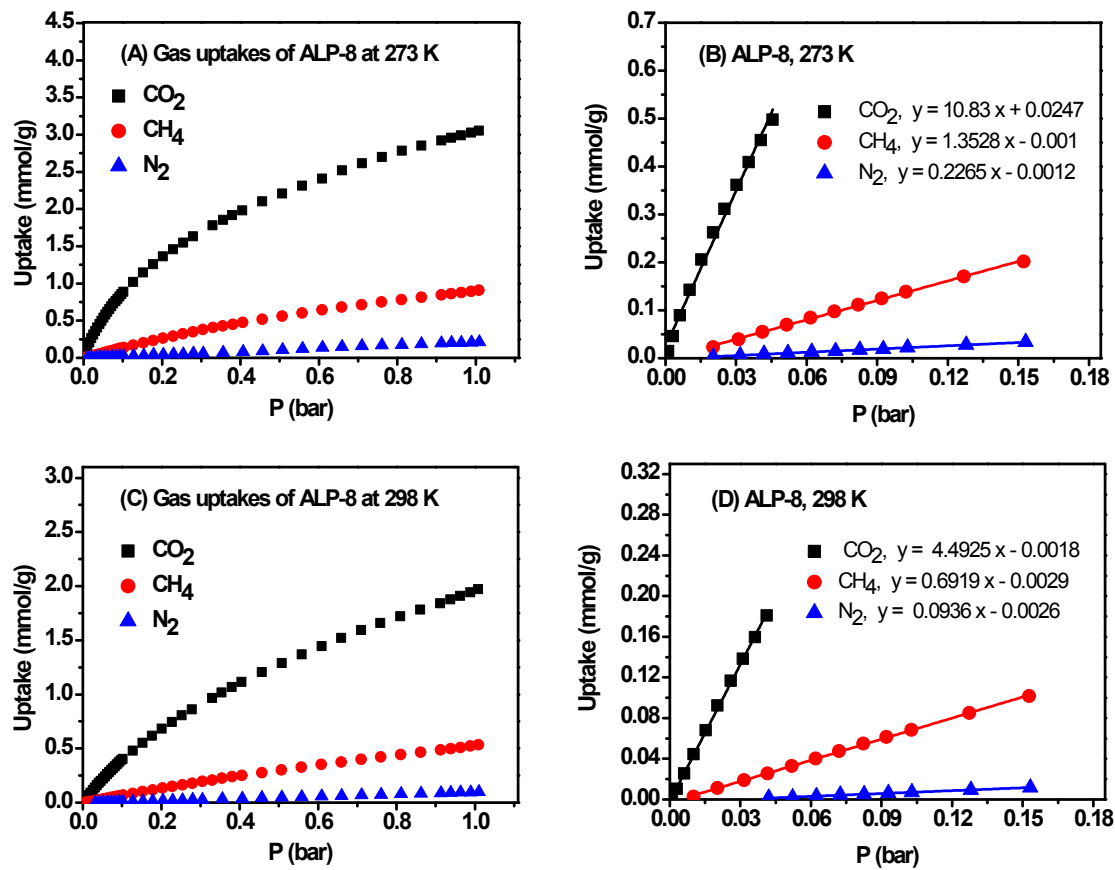


**Table S6.** Initial slope selectivity of ALPs.

Polymer	CO <sub>2</sub> /N <sub>2</sub> Selectivity <sup>a</sup>		CO <sub>2</sub> /CH <sub>4</sub> Selectivity <sup>a</sup>		Reference
	273 K	298 K	273 K	298 K	
ALP-1	35	27	6	5	<sup>1</sup>
ALP-5	51	41	9	7	This Work
ALP-6	46	47	8	6	This Work
ALP-7	47	43	8	7	This Work
ALP-8	48	48	8	6	This Work

<sup>a</sup>(mol mol<sup>-1</sup>).

## References

1. P. Arab, M. G. Rabbani, A. K. Sekizkardes, T. İslamoğlu and H. M. El-Kaderi, *Chem. Mater.*, 2014, **26**, 1385-1392.
2. H. A. Patel, S. H. Je, J. Park, D. P. Chen, Y. Jung, C. T. Yavuz and A. Coskun, *Nat. Commun.*, 2013, **4**, 1357.
3. J. Lu and J. Zhang, *J. Mater. Chem. A.*, 2014, **2**, 13831-13834.